Rapid and ultrasensitive electrochemical detection of DNA methylation for ovarian cancer diagnosis

Author:
Chen, D; Wu, Y; Tilley, RD; Gooding, JJ

Publication details:
Biosensors and Bioelectronics
v. 206
Medium: Print-Electronic
0956-5663 (ISSN); 1873-4235 (ISSN)

Publication Date:
2022-06-15

Publisher DOI:
https://doi.org/10.1016/j.bios.2022.114126

Rapid and ultrasensitive electrochemical detection of DNA methylation for ovarian cancer diagnosis

Dongfei Chen[a], Yanfang Wu[a]*, Richard D. Tilley[b], and J. Justin Gooding[a]*

[a] School of Chemistry, Australian Centre for NanoMedicine, and Australian Research Council Centre of Excellence in Convergent Bio-Nano Science and Technology, The University of New South Wales, Sydney, New South Wales 2052, Australia

[b] School of Chemistry, Australian Centre for NanoMedicine, Electron Microscope Unit, Mark Wainwright Analytical Centre, The University of New South Wales, Sydney, NSW 2052, Australia

* Corresponding author: yanfang.wu@unsw.edu.au (Y. Wu); justin.gooding@unsw.edu.au (J. J. Gooding)

Abstract

Alterations in DNA methylation, a stable epigenetic marker, are important components in the development of cancer. It is vital to develop diagnostic systems with the ability to rapidly quantify DNA methylation with high sensitivity and selectivity. However, the analysis of DNA methylation must address two main challenges: (i) ultralow abundance and (ii) differentiating methylated cytosine from normal cytosine on target DNA sequence in the presence of an overwhelming background of circulating cell-free DNA. Here we report the development of an ultrasensitive and highly-selective electrochemical biosensor for the rapid detection of DNA methylation in blood. The sensing of DNA methylation involves the hybridization on a network of probe DNA modified gold-coated magnetic nanoparticles (DNA-Au@MNPs) complementary to target DNA, and subsequently enzymatic cleavage to differentiate methylated DNA strands from corresponding unmethylated DNA strands. The biosensor presents a dynamic range from 2 aM to 20 nM for 110 nucleotide DNA sequences containing a single-site methylation with the lowest detected concentration of 2 aM. This DNA-Au@MNPs based sensor provides a promising method to achieve 35 min response time and minimally invasive diagnosis of ovarian cancer.

Keywords

DNA methylation; Electrochemistry; Liquid biopsy; Gold-coated magnetic nanoparticle; Biosensor

1. Introduction

Epigenetic modification of nucleic acids is commonly referred to as a genomic mechanism that can reversibly influence gene expression without altering DNA sequences. It has been revealed that epigenetic modifications play an important role in regulating gene expression and silencing transposons, including hypomethylation of oncogenes and hypermethylation of tumor suppressor genes (Bock et al. 2010; Cokus et al. 2008; Irizarry et al. 2009). The occurrence of aberrant epigenetic modification is closely linked with multiple diseases, especially carcinogenesis (Portela and Esteller 2010; Robertson 2005). DNA methylation is a mammalian stable epigenetic marker, resulting from the addition of a methyl group at the fifth carbon of the cytosine base in the CpG dinucleotides of DNA (Laird 2010; Smith and Meissner 2013). Using DNA methylation as a diagnostic biomarker presents several advantages over other biomarkers, including its relatively good stability, both *in vivo* and *ex vivo*. DNA methylation occurs early in tumorigenesis and is highly pervasive across tumor types. It is associated with the origin of some cancers (Guo et al. 2018; Locke et al. 2019). It has been shown that DNA methylation as a blood-derived biomarker, has the potential to detect ovarian cancer up to two years in advance of clinical diagnosis (Widschwendter et al. 2017). Thus, the analysis of DNA methylation has emerged rapidly as a promising tool with many potential clinical applications in oncology. However, two main challenges need to be resolved for an effective sensor for detecting methylated DNA. Firstly, there is only a trace amount of DNA methylation in clinical samples, although changes in DNA methylation emerge in the early stages of cancer. The level of circulating tumor DNA methylation was shown to be as low as 0.05% of the overall amount of cell-free DNA (cfDNA) circulating in the bloodstream (Luo et al. 2021). Note that the concentration of cfDNA typically ranges from 0 to 50 ng/mL, which is already found at ultalow levels (Lam et al. 2020; Widschwendter et al. 2017). As such, it is extremely difficult to isolate methylated DNA from cfDNA with current technologies. Secondly, DNA methylation also faces the challenge of making distinctions between cfDNA and genomic DNA in the early diagnosis of tumors. Bisulfite conversion has emerged as a gold standard method for the analysis of DNA methylation (Li et al. 2009; Liu et al. 2019). With this method,

DNA needs to be treated with sodium bisulfite, leaving the methylated cytosine (mC) unaffected but converting the unmethylated cytosine (C) to uracil (U) which will further be turned into thymine (T) after PCR amplification. After the chemical reaction by sodium bisulfite and PCR amplification, the information of methylation is transferred into the information of sequence, enabling the detection of DNA methylation with a single base resolution. It would be ideal however to be able to avoid the sample preparation required prior to sensing that is necessary with the bisulfite strategy.

Recently, a number of detection strategies for DNA methylation have been reported, which can be classified into three categories. (1) Direct electrochemical oxidation-based assay. For example, Niwa et al. employed a nanocarbon film electrode for the quantitative measurement of both C and mC by measuring the difference in potential peak caused by cytosine methylation (Kato et al. 2008). Although direct electrochemical oxidation of DNA is a simple method for DNA methylation detection, concern arises as the oxidation potential of thymine (T) is almost the same as that of mC, resulting in difficulty in detection of DNA methylation in the presence of T. (2) Biological recognition-based assay. For example, Ai et al. developed an electrochemical immunosensor to detect DNA methylation by taking advantage of methyl-CpG-binding domain (MBD) which can recognize symmetrical methylated double-stranded DNA. The immunosensor presented a dynamic range from 5 to 500 pM with a detection limit of 0.17 pM (Xu et al. 2014). (3) Restriction endonuclease-based assay. For example, Hou et al. described a detection method for DNA methylation by coupling restriction endonucleases (BstUI/HhaI) with a recombinase polymerase amplification-assisted CRISPR/Cas13a system. The BstUI/HhaI restriction enzyme can digest unmethylated DNA, whereas the cleavage activity of BstUI/HhaI restriction enzyme is blocked in the presence of DNA methylation. The fabricated sensor was shown to present a dynamic range from 200 aM to 20 pM with a detection limit of 86.4 aM with the assay time being over 2 hours (Wang et al. 2021). In this regard, an important milestone for the implementation of DNA methylation assays into clinical

practice is to develop rapid, highly sensitive and selective sensing technologies for detecting ultralow amounts of methylated DNA directly in clinical samples.

The twin challenges of low detection limits and rapid analysis time are often contradictory (Wu et al. 2019). In general, the lower the detection limit, the longer the analysis time required, and vice versa. In this regard, the concept of dispersible electrodes rises to these twin challenges (Moraes Silva et al. 2016). Dispersible electrodes are gold-coated magnetic nanoparticles (Au@MNP) that are modified with biorecognition molecules to selectively detect the analyte of interest. The Au@MNPs are dispersed throughout a sample to capture the target analyte and then brought back to a macroelectrode under magnetic control to allow electrochemical detection of the amount of analyte capture. This simple idea of breaking the electrode up into tiny nanoscale particles that seek out the analyte rather than the conventional paradigm of making the analyte find the sensor has successfully been shown to give ultrasensitive detection of a variety of analytes, including metal ions, proteins, microRNAs and circulating tumor DNAs (Chen et al. 2021; Chuah et al. 2012; Goon et al. 2010; Tavallaie et al. 2018). This concept allows the preconcentration and detection of analyte species to occur with the same gold-coated magnetic nanoparticle but at different times, solutions, and interfaces. The dispersible electrode concept leads to significantly shortened analysis times and lowered detection limits. However, this detection method is not capable of directly analyzing DNA methylation due to that DNA sequences containing 5-methylcytosines do not interfere with Watson–Crick base pairing (Dantas Machado et al. 2015). To differentiate 5-methylcytosine from normal cytosine in a DNA target, one possible sensing strategy is to couple the dispersible electrodes system with the employment of restriction endonucleases. For instance, HhaI restriction endonuclease can specifically recognize and cleave (↓) the symmetrical sequence 5’-GCG↓C-3’ in DNA duplexes; a cleavage that is blocked when the internal cytosine is methylated (Vardimon and Rich 1984).

The purpose of the study presented herein was to combine the dispersible electrodes concept with the use of HhaI restriction endonuclease to develop an electrochemical sensor for the detection of DNA methylation. The key novelty of the work is the application of the dispersible electrodes concept to a new class of analyte, methylated DNA, without requiring significant sample preparation such that the levels of methylated DNA directly in blood can be monitored. To achieve this a 110 nucleotide DNA sequence containing a single-site methylation, indicative of ovarian cancer, was chosen as the model analyte (Widschwendter et al. 2017). The Au@MNPs were modified with thiolated probe DNA molecules that are complementary to the methylated DNA target. Ferricyanide was used as the redox probe to generate electrochemical signals, subject to the quantity of target DNA hybridized on the surface of DNA-Au@MNPs. The electrochemical behavior of the DNA-Au@MNPs was investigated by square wave voltammetry (SWV). Surface passivation on gold macroelectrode surface with thiolated DNA and mercaptohexanol (MCH) was performed to enhance the sensor sensitivity, according to our previous experience. This sensor was employed to detect various concentrations of the 110 nucleotide DNA sequence with a single-site methylation in buffer solutions and human blood samples with a 35 min response time. The dynamic range, detection limit, and sensor specificity of the developed sensor were evaluated as well.

2. Experimental section

2.1 Materials and apparatus

All oligonucleotides, shown in Table S1 in supporting information, were synthesized by Integrated DNA Technologies (IDT). 6-mercapto-1-hexanol (MCH), sodium chloride (NaCl), tris(2-carboxyethyl)phosphine hydrochloride (TCEP), potassium hexacyanoferrate (III) ($K_3[Fe(CN)_6]$), Dulbecco's phosphate-buffered saline (PBS) were acquired from Sigma-Aldrich. HhaI restriction endonuclease and 10x CutSmart Buffer were purchased from New England Biolabs (Sydney, Australia). Sodium phosphate monobasic (NaH_2PO_4), sodium phosphate dibasic (Na_2HPO_4) and ethanol were purchased from Chem-Supply Pty. Ltd (Australia). Milli-

Q water (~18 MΩ cm, Millipore, Australia) was used to prepare experimental solutions. Blood used in this study was purchased from Australia Red Cross.

A CHI660E electrochemical workstation (CH Instruments, Inc.) was used to measure square wave voltammograms (SWVs). A three-electrode system was equipped for electrochemical measurements, using bare gold foil as the working electrode, Ag/AgCl (3.0 M KCl) as the reference electrode and platinum wire as the counter electrode.

2.2 Surface modification of gold foil

The gold foil was polished by alumina polishing powders with the particle size of 1.0, 0.3 and 0.05 μm, respectively. After ultrasonically washing in Milli-Q water, the electrode was rinsed successively with absolute alcohol and Milli-Q water and then dried by nitrogen. Prior to the incubation, 50 μL of 4 μM probe DNA was mixed with 2 μL of 1mM TCEP for 1 h. The thiolated probe DNA monolayer on gold foil was prepared by incubating the cleaned gold electrode in the solution of probe DNA for 8 h. A 40 μL aliquot of 2 mM MCH was mixed with 8 μL of 10 mM TCEP for 1 h. The above gold substrate was then immersed into the reduced MCH solution for 3 h. Before electrochemical measurement, the gold foil was rinsed thoroughly by Milli-Q water.

2.3 Surface modification of Au@MNPs with probe DNA

Prior to the modification, the disulfide bond of the probe DNA was reduced by adding 1 mM TCEP to 100 nM thiolated probe DNA. The mixture was kept for 1 h at room temperature. To immobilize probe DNA onto the surface of Au@MNPs, redispersed 10 μL Au@MNPs with a concentration of 1.56×10^{10} particles per mL were added to freshly prepared 100 nM thiolated probe DNA solution and incubated while mixing gently in a rotating wheel, followed by four dropwise additions of 1.0 M NaCl solution to obtain a final concentration of 0.15 M. Then incubating on a rotating wheel overnight, probe DNA modified Au@MNPs were separated

from the supernatant solution by 5 min centrifugation at 5000 revolutions per minute (rpm). Modified nanoparticles were rinsed once using phosphate-buffered saline.

2.4 Hybridization procedure

Different concentrations of target DNA were prepared by serial dilution of stock DNA solution. To hybridize the probe DNA-Au@MNPs with target DNA, 100 µL of target DNA in appropriate concentrations (0 aM, 2 aM, 200 aM, 20 fM, 2 pM, 200 pM and 20 nM) was added to the freshly prepared DNA-Au@MNPs and the mixture was kept for 20 min in the rotating wheel at room temperature. Then, the hybridized DNA-Au@MNPs were separated from the supernatant solution by centrifugal method (5000 revolutions per minute for 5 min) and rinsed once using phosphate-buffered saline solution. The hybridized DNA-Au@MNPs was followed by enzymatic cleavage with HhaI restriction endonuclease (20,000 units/mL). It was carried out in a 50 µL of the mixture containing 1x CutSmart buffer (including 50 mM potassium acetate, 20 mM Tris-acetate, 10 mM magnesium acetate, 100 µg/mL recombinant albumin), 20 U of HhaI and the hybridized DNA-Au@MNPs. The mixture was kept at 37 ^{o}C for 15 min for the digestion treatment in which the unmethylated target DNA was digested but not the methylated target DNA.

2.5 Electrochemical measurement

Signal changes corresponding to a specific target were calculated with background-subtracted SWVs: % change in current = ($I_{ssDNA\text{-}Au@MNPs} - I_{dsDNA\text{-}Au@MNPs}$) / $I_{ssDNA\text{-}Au@MNPs}$ * 100% (where $I_{ssDNA\text{-}Au@MNPs}$ = current before hybridization, $I_{dsDNA\text{-}Au@MNPs}$ = current after hybridization).

3. Results and discussion

Combining the selective capture capacity of ‘dispersible electrodes’ with sequence-specific restriction endonuclease HhaI, an ultrasensitive and highly selective system was established for the detection of DNA methylation levels directly in human blood with a broad dynamic range. The Au@MNPs used in this study were synthesized according to our previously

reported procedure (Goon et al. 2009). A detailed characterization of Au@MNPs has been reported in our previous study (Chen et al. 2021). The sensing principle of the system is illustrated in Figure 1. The surface of the Au@MNP was modified with thiolated probe DNA sequence (43 nucleotides), complementary to a portion of the 110 nucleotide DNA target. After exposing the DNA-Au@MNPs to methylated or unmethylated DNA target for 20 min, the hybridized DNA-Au@MNPs were magnetically isolated from the sample solution followed by the treatment with HhaI restriction endonuclease for 15 min. Then dsDNA-Au@MNPs were collected by a magnet and redispersed into phosphate-buffered saline (pH 7.4) containing 0.5 mM potassium ferricyanide ($K_3[Fe(CN)_6]$) in a custom-made glass cell. Using a magnet, the dsDNA-Au@MNPs were brought to the gold electrode surface modified with 22 nucleotides thiolated DNA and mercaptohexanol (MCH) for electrochemical measurements. As shown previously, a self-assembled monolayer of thiolated DNA and MCH on the underlying gold electrode would induce a larger change in current, and hence give the sensor a greater sensitivity, compared to that when there was no such surface modification on the electrode (Chen et al. 2021). The sequences of all DNA strands employed in this study can be seen in Table S1 in supporting information.

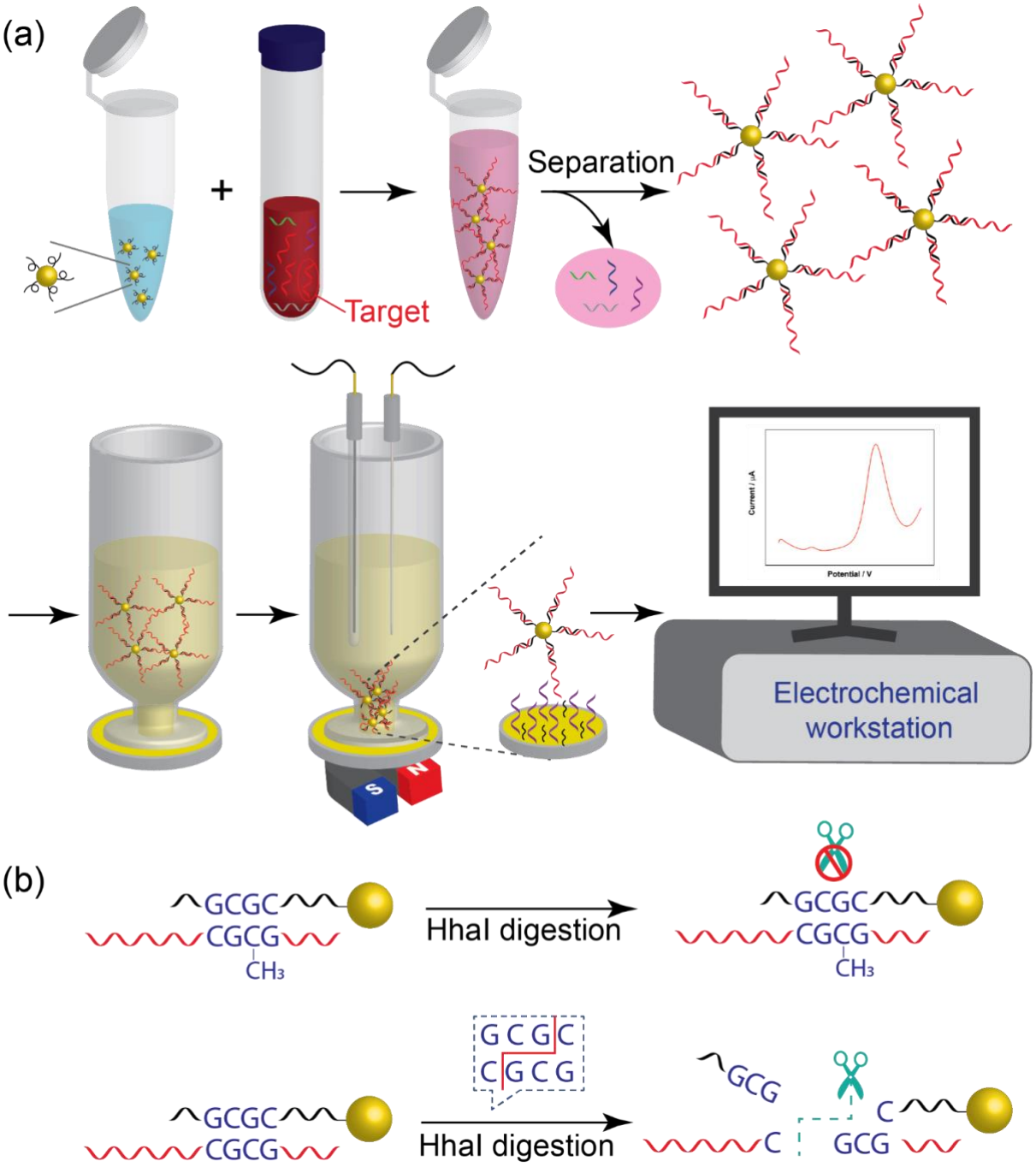

Figure 1. Schematic illustration of the detection of DNA methylation based on nucleic acid hybridization on a network of gold-coated magnetic nanoparticles. (a) Workflow for the measurement of methylated DNA. (b) Principle of the specific detection of DNA methylation. Methylated DNA survived HhaI digestion, whereas unmethylated DNA was digested by HhaI restriction enzyme. The use of HhaI restriction endonuclease facilitates the specific and sensitive detection of 110 nucleotide DNA target with a single-site 5-methylcytosine.

The electrochemical response of the described sensor is shown in Figure 2, where after the DNA-Au@MNPs (black curve in Figure 2) were hybridized with target DNA, a decrease in SWV current was observed related to the detection of 20 nM methylated target DNA (blue curve in Figure 2). The suppression in the peak current after hybridization was due to the formation of duplex DNA affecting the electronic communication among nanoparticles in the network system. The steric hindrance and charge repulsion effects also increased because more negative charges appeared on the surface of hybridized DNA-Au@MNPs. The faradaic electrochemistry of the $[Fe(CN)_6]^{3-}$ was therefore hindered and a lower current was observed. In the presence of HhaI restriction endonuclease, the unmethylated DNA captured on the DNA-Au@MNPs was cleaved into smaller fragments followed by their releasing from the nanoparticle surface. As a result, improved electronic communication in the nanoparticles network and less negative charges on the surface of cleaved dsDNA-Au@MNPs recovered the electrochemical signals for unmethylated DNA-Au@MNPs (red curve in Figure 2). Cyclic voltammograms and Nyquist diagrams of the sensor at different stages are presented in Figure S1. The utilization of the Hhal restriction enzyme caused no significant change in the sensor response for detecting methylated DNA target compared to when no Hhal was employed (Figure S2). This observation shows that if there is any nonspecific adsorpton of the restriction endonuclease Hhal adsorbed onto the hybridized DNA modified gold-coated magnetic nanoparticles it was not influencing the current response. The importance of introducing $K_3[Fe(CN)_6]$ into the detection solution to amplify the sensing signals for DNA methylation detection was demonstrated as well (Figure S3).

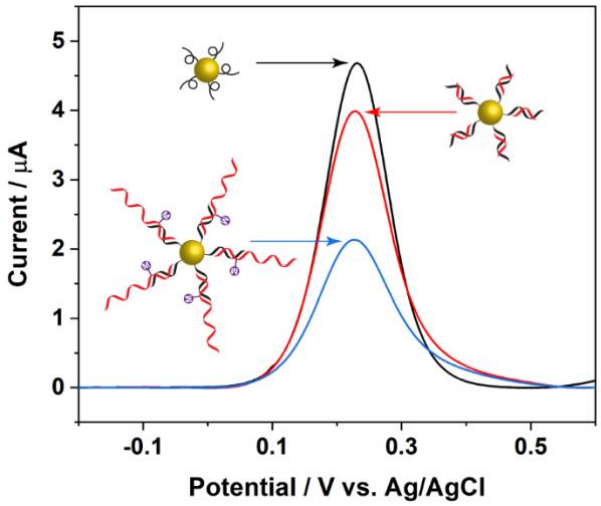

Figure 2. Square wave voltammograms (SWVs) obtained from ssDNA-Au@MNPs (black) after exposing the sensor to 20 nM methylated target DNA (blue) and 20 nM unmethylated target DNA (red), followed by HhaI restriction enzymatic cleavage. The gold foil was pre-modified with thiolated DNA (22 nucleotides) and mercaptohexanol (MCH). Electrolyte solution was 0.5 mM $K_3[Fe(CN)_6]$ in phosphate-buffered saline (pH 7.4). The frequency and pulse amplitude of SWVs were 2 Hz and 25 mV, respectively.

To examine the concentration-dependent sensor response to methylated DNA target, the lowest detected concentration and dynamic range of the sensor were evaluated by detecting different concentrations of the 110 nucleotides methylated DNA in phosphate buffered saline and 50% human blood. Under the applied experimental conditions, it is unlikely that the oligonucleotides used in this study present any stable secondary structure. Recently, there was a discussion about the appropriateness of using semilogarithmic calibration plots to show sensor responses (Kong et al. 2021; Urban 2020). As such, in this study we chose to report data using both linear and non-linear calibration data sets. The dependence of the change in peak current in the SWVs on the logarithmic concentration of methylated DNA target is shown in Figure 3. The linear regression equation was found to be Y = 4.286X + 89.279 with a standard error of the regression of 0.74 for the methylated DNA target spiked in buffer solutions. A dynamic range from 2 aM to 20 nM covering 10 orders of magnitude was achieved

with the lowest detected concentration of 2 aM. Furthermore, we also investigated the concentration-dependent current changes in blood samples. The blood samples used in this study were spiked with different concentrations of the methylated DNA target. The detection performance in 50% human whole blood was evaluated. The corresponding linear regression equation was Y = 4.1793X + 84.703 with a standard error of the regression of 1.09, which is comparable with the performance in buffer solutions, indicating the potential for this sensor in the direct analysis of DNA methylation from complex biological samples. The non-linear calibration curves for the sensor responding to different concentrations of methylated DNA target in buffer solutions and 50% human blood are presented in Figure S4 in supporting information.

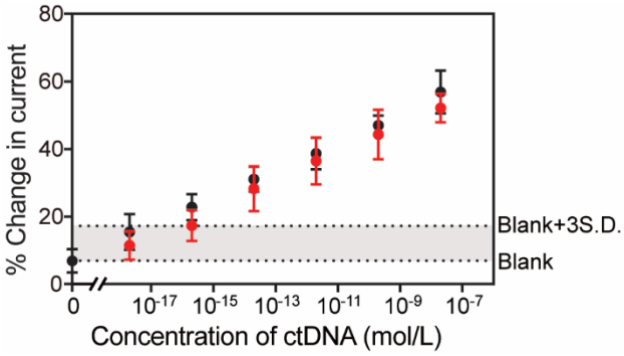

Figure 3. The dependence of hybridization-induced current change from SWVs upon 110 nucleotides methylated target DNA (0 aM, 2 aM, 200 aM, 20 fM, 2 pM, 200 pM and 20 nM) spiked in phosphate-buffered saline (black data points) and 50% whole blood (red data points). Two dash lines are provided to indicate the levels of the average blank and the three times standard deviation above the averaged blank. Error bars represent standard deviations from 5 independent measurements.

The selectivity of the sensor was explored by comparing the electrochemical responses of methylated DNA target from a pure matrix of methylated target DNA and a mixture of both background cfDNA and methylated DNA target. We evaluated the sensor performance in the specific detection of 20 fM methylated target DNA in the presence of a 101 nucleotide DNA strand of non-complementary sequence (utilized as the background cfDNA) with a significantly

higher concentration of 20 nM in phosphate-buffered saline and 50% human blood (Figure 4). In the phosphate-buffered saline solution, an average change of (32.5 ± 5.0)% decrease in current was observed after hybridization with 20 fM methylated DNA. If both 20 fM methylated DNA and 20 nM non-complementary background cfDNA was added there was still a very similar change in current of (30.4 ± 5.4)% which illustrates the abiity of the method to delect the target sequence in the presence of other nucleic acids. Furthermore, the current change observed in 50% blood samples were (31.5 ± 4.7)% and (30.9 ± 5.9)% for target only and the target mixed with noncomplementary DNA, respectively. The performance of this proposed sensor in 50% blood sample showed only a minimal difference relative to that in phosphate-buffered saline, indicating the robustness of the sensor even in complex blood environment. Taken together, our sensing system demonstrated a high selectivity to the methylated DNA target regardless of sample medium and thus presents great potential to be employed for detecting trace amount of methylated DNA molecules in complex biofluids with the presence of an overwhelming background of circulating cfDNA. A comparison of the sensing characteristics for the developed sensor and other sensors reported for the detection of DNA methylation is presented in Table S2.

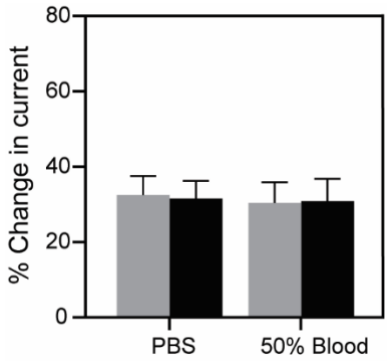

Figure 4. Anti-interference of the developed sensor for the detection of methylated target DNA in the presence of high abundance cell-free DNA with non-complementary sequence in phosphate-buffered saline (PBS) and 50% whole blood. Grey columns indicate the percentage changes in current for measurements of 20 fM methylated DNA sequence in PBS, whereas black columns represent the percentage changes in current for measurements at samples containing both 20 fM methylated DNA sequence and 20 nM 101 nucleotide non-

complementary DNA sequence (utilized as the background cell-free DNA) in 50% whole blood. Error bars represent standard deviations from 5 independent measurements.

The reproducibility of the sensor (Figure S5) was determined as the relative standard deviation (RSD) of five independent parallel experiments in the same conditions, slight variation in the current change was calculated to be 3.6% and 5.4% obtained from ssDNA-Au@MNPs and after exposing the ssDNA-Au@MNPs to 200 pM methylated target DNA in 50% human blood, respectively. The results indicated a good reproducibility of the fabricated sensor. Furthermore, to test the repeatability of the fabricated sensor (Figure S5), six repetitive measurements were performed using a single electrode. Relative standard deviation (RSD) was calculated to be 3.9% and 4.3% for six repetitive SWV scanning obtained from ssDNA-Au@MNPs and after exposing the sensor to 2 aM methylated target DNA, respectively. The results demonstrated a satisfactory repeatability of the sensor. In addition to this, the storage stability of the proposed sensor (Figure S6) was also investigated. The sensor was stored at 4 ^{o}C and tested every 5 h. The peak current value barely declined and retained at 97.2% of its initial current after 35 h, indicating sufficient stability of the sensor

4. Conclusions

In this study, an ultrasensitive and highly-selective electrochemical sensor was developed for the rapid detection of DNA methylation directly in blood samples. In combination with dispersible electrodes system and HhaI restriction enzyme, as low as 2 aM of 110 nucleotide methylated DNA with a single-site methylation, a diagnostic biomarker for ovarian cancer, can be electrochemically detected. The sensitivity and lowest detected concentration of this sensor compare favorably with the reported state-of-the-art DNA methylation sensors (Feng et al. 2020; Feng et al. 2019; Huang et al. 2019; Sun et al. 2018). The most important feature of our biosensing strategy is that it can effectively identify trace amounts of methylated DNA from high concentration of cell-free DNA even in complex blood samples without extensive sample preparation needed by bisulfite and PCR amplification detection methods for extracting DNA

from blood or tissue biopsy samples (Sina et al. 2019). In addition to this, the approach enables rapid analysis of DNA methylation in a response time of 35 min, compared to that of 3–5 h in other studies (Chen et al. 2019; Huang et al. 2019; Wang et al. 2021). We believe that this rapid and simple approach with the excellent sensitivity and specificity would potentially be an excellent companion diagnostic detection for ovarian cancer in clinic. Furthermore, the sensing system is not limited to the detection of DNA methylation with a specific sequence of 5'-GCGC-3', instead it could be extended to diagnose other DNA sequences coupled with the employment of else sequence-specific restriction endonuclease enzymes.

Acknowledgments

This research was supported by the National Health and Medical Research Council Investigator Award (APP1196648).

References

Bock, C., Tomazou, E.M., Brinkman, A.B., Muller, F., Simmer, F., Gu, H., Jager, N., Gnirke, A., Stunnenberg, H.G., Meissner, A., 2010. Nat. Biotechnol. 28, 1106-1114.

Chen, D.F., Wu, Y.F., Hoque, S., Tilley, R.D., Gooding, J.J., 2021. Chem. Sci. 12, 5196-5201.

Chen, X., Huang, J., Zhang, S., Mo, F., Su, S., Li, Y., Fang, L., Deng, J., Huang, H., Luo, Z., Zheng, J., 2019. ACS Appl. Mater. Interfaces 11, 3745-3752.

Chuah, K., Lai, L.M., Goon, I.Y., Parker, S.G., Amal, R., Gooding, J.J., 2012. Chem. Commun. 48, 3503-3505.

Cokus, S.J., Feng, S., Zhang, X., Chen, Z., Merriman, B., Haudenschild, C.D., Pradhan, S., Nelson, S.F., Pellegrini, M., Jacobsen, S.E., 2008. Nature 452, 215-219.

Dantas Machado, A.C., Zhou, T., Rao, S., Goel, P., Rastogi, C., Lazarovici, A., Bussemaker, H.J., Rohs, R., 2015. Brief. Funct. Genomics 14, 61-73.

Feng, Q., Qin, L., Wang, M., Wang, P., 2020. Biosens. Bioelectron. 149, 111847.

Feng, Q., Wang, M., Qin, L., Wang, P., 2019. ACS Sens. 4, 2615-2622.

Goon, I.Y., Lai, L.M., Lim, M., Amal, R., Gooding, J.J., 2010. Chem. Commun. 46, 8821-8823.

Goon, I.Y., Lai, L.M.H., Lim, M., Munroe, P., Gooding, J.J., Amal, R., 2009. Chem. Mater. 21, 673-681.

Guo, W., Zhu, L., Yu, M., Zhu, R., Chen, Q., Wang, Q., 2018. Clin. Epigenetics 10, 142.

Huang, J., Zhang, S., Mo, F., Su, S., Chen, X., Li, Y., Fang, L., Huang, H., Deng, J., Liu, H., Yang, X., Zheng, J., 2019. Biosens. Bioelectron. 127, 155-160.

Irizarry, R.A., Ladd-Acosta, C., Wen, B., Wu, Z., Montano, C., Onyango, P., Cui, H., Gabo, K., Rongione, M., Webster, M., Ji, H., Potash, J., Sabunciyan, S., Feinberg, A.P., 2009. Nat. Genet. 41, 178-186.

Kato, D., Sekioka, N., Ueda, A., Kurita, R., Hirono, S., Suzuki, K., Niwa, O., 2008. J. Am. Chem. Soc. 130, 3716-3717.

Kong, D., Zhao, J., Tang, S., Shen, W., Lee, H.K., 2021. Anal. Chem. 93, 12156-12161.

Laird, P.W., 2010. Nat. Rev. Genet. 11, 191-203.

Lam, D., Luu, P.L., Song, J.Z., Qu, W., Risbridger, G.P., Lawrence, M.G., Lu, J., Trau, M., Korbie, D., Clark, S.J., Pidsley, R., Stirzaker, C., 2020. Clin. Epigenetics 12, 90.

Li, M., Chen, W.D., Papadopoulos, N., Goodman, S.N., Bjerregaard, N.C., Laurberg, S., Levin, B., Juhl, H., Arber, N., Moinova, H., Durkee, K., Schmidt, K., He, Y., Diehl, F., Velculescu, V.E., Zhou, S., Diaz, L.A., Jr., Kinzler, K.W., Markowitz, S.D., Vogelstein, B., 2009. Nat. Biotechnol. 27, 858-863.

Liu, Y., Siejka-Zielinska, P., Velikova, G., Bi, Y., Yuan, F., Tomkova, M., Bai, C., Chen, L., Schuster-Bockler, B., Song, C.X., 2019. Nat. Biotechnol. 37, 424-429.

Locke, W.J., Guanzon, D., Ma, C., Liew, Y.J., Duesing, K.R., Fung, K.Y.C., Ross, J.P., 2019. Front. Genet. 10, 1150.

Luo, H., Wei, W., Ye, Z., Zheng, J., Xu, R.H., 2021. Trends Mol. Med. 27, 482-500.

Moraes Silva, S., Tavallaie, R., Sandiford, L., Tilley, R.D., Gooding, J.J., 2016. Chem. Commun. 52, 7528-7540.

Portela, A., Esteller, M., 2010. Nat. Biotechnol. 28, 1057-1068.

Robertson, K.D., 2005. Nat. Rev. Genet. 6, 597-610.

Sina, A.A., Carrascosa, L.G., Trau, M., 2019. Trends Mol. Med. 25, 955-966.

Smith, Z.D., Meissner, A., 2013. Nat. Rev. Genet. 14, 204-220.

Sun, Y., Sun, Y., Tian, W., Liu, C., Gao, K., Li, Z., 2018. Chem. Sci. 9, 1344-1351.

Tavallaie, R., McCarroll, J., Le Grand, M., Ariotti, N., Schuhmann, W., Bakker, E., Tilley, R.D., Hibbert, D.B., Kavallaris, M., Gooding, J.J., 2018. Nat. Nanotechnol. 13, 1066-1071.

Urban, P.L., 2020. Anal. Chem. 92, 10210-10212.

Vardimon, L., Rich, A., 1984. Proc. Natl. Acad. Sci. 81, 3268-3272.

Wang, X., Zhou, S., Chu, C., Yang, M., Huo, D., Hou, C., 2021. ACS Sens. 6, 2419-2428.

Widschwendter, M., Zikan, M., Wahl, B., Lempiainen, H., Paprotka, T., Evans, I., Jones, A., Ghazali, S., Reisel, D., Eichner, J., Rujan, T., Yang, Z., Teschendorff, A.E., Ryan, A., Cibula, D., Menon, U., Wittenberger, T., 2017. Genome Med. 9, 116.

Wu, Y.F., Tilley, R.D., Gooding, J.J., 2019. J. Am. Chem. Soc. 141, 1162-1170.

Xu, Z., Yin, H., Huo, L., Zhou, Y., Ai, S., 2014. Sens. Actuators B Chem. 192, 143-149.F